Void percolation and conduction of overlapping ellipsoids

Y. B. Yi
Department of Engineering, University of Denver, Denver, Colorodo 80208, USA
(Received 7 May 2006; revised manuscript received 17 July 2006; published 13 September 2006)

The void percolation and conduction problems for equisized overlapping ellipsoids of revolution are investigated using the discretization method. The method is validated by comparing the estimated percolation threshold of spheres with the precise result found in literature. The technique is then extended to determine the threshold of void percolation as a function of the geometric aspect ratio of ellipsoidal particles. The finite element method is also applied to evaluate the equivalent conductivity of the void phase in the system. The results confirm that there are no universalities for void percolation threshold and conductivity in particulate systems, and these properties are clearly dependent on the geometrical shape of particles. As a consequence, void percolation and conduction associated with ellipsoidal particles of large aspect ratio should be treated differently from spheres.

DOI: 10.1103/PhysRevE.74.031112 PACS number(s): 64.60.Ak, 05.45.Df

I. INTRODUCTION

Percolation is typically associated with conduction problems in heterogeneous materials. It is a phenomenon in which there exists at least one domain-spanning conductive pathway in a multiphase material. (One of the phases could be the void space.) In a system of overlapping particles, for example, when the particle density exceeds a certain threshold, the particles will form large clusters that span the whole material domain. Although the concept of percolation was originally introduced to study fluid flow in porous media [1], it has a wide application in other areas as well. For example, it is evident that the determination of mathematical and physical characteristics associated with percolation phenomena is important in studying fibrous or particulate engineered materials, such as advanced batteries and carbon nanotubes for mechanical [2], filtration [3], and conductive [4,5] properties.

Two methods—analytical approach and Monte Carlo simulation—have been extensively used to study percolation phenomena. The earlier efforts were primarily concentrated on seeking the analytical solutions for percolation thresholds of fixed lattices in two or three dimensions [6]. In the last decades, with the aid of advanced computer technologies, many researchers made great efforts in solving continuum percolation problems related to particles randomly distributed in space. Pike and Seager [7], for example, reported Monte Carlo simulation results for the effects of various probabilistic and deterministic bonding parameters in sphere continuum percolation. Some researchers attempted to use the series expansion technique [8] and the integral method [9] to estimate the percolation properties for continuum percolation, via checking the convergence of the mean cluster size expressed in the form of a power series. However, the requirement of considerable computational effort poses a major hurdle to its practical application. In general, Monte Carlo simulation method has been proved more efficient in determining percolation properties of continuum percolation problems, especially for nonspherical particles [10].

For conduction problems in multiphase materials, analytical approximations using the effective medium theories can readily be found in literature [11,12]. However, the Monte Carlo simulation method is much easier to implement and has thus been used more extensively. For example, in Cheng and Sastry's work [13], fibrous materials relevant to battery technologies were examined for their conductive properties via modeling the material system as a fibrous network. They found that the equivalent conductivity of the system is strongly dependent on fiber aspect ratio.

Typically, percolation and conduction are relative to the material media in a multiphase system. When the interconnection of the void phase is in interest, the percolation is called "void percolation" or "Swiss-cheese percolation" [14]. This type of percolation is closely related to the fluid flow through porous media. However, much less attention has thus far been paid to void percolation than the traditional percolation problems. This is partly due to the complexity in mathematical expressions of the connection functions in void percolation problems. Even for the simplest case of monodisperse spheres, it was not until very recently that researchers realized that the void percolation problem can be simplified by mapping the system to a bond network associated with the Voronoi tessellation of the sphere centers [15]. Because of the increased complexity involved in computing the Voronoi tessellation and the memory requirement to store the data structures, the numerical accuracy for the computed percolation threshold was originally not satisfactory. However, thanks to the advancement of computer technology and the refinement of the solution method, the results have been improved significantly over the last decade. For example, Rintoul [16] reported a technique using scaling theories to obtain a very precise result (0.0301 ± 0.0003) for percolation threshold of mondisperse sphere systems.

Some researchers proposed that there exist universal constants for void percolation thresholds and other conductive properties for spheres of different size and distribution [17]. Rintoul's work, however, overturned this conjecture, by showing the differences in the percolation threshold between monodisperse and bidisperse sphere systems. Although it is helpful investigating the fundamental characteristics of void percolation for spheres, an interesting question arises: does the geometric shape of nonspherical particles also affect the

percolation properties? Previous work on overlapping ellipsoidal systems showed that the aspect ratio of particles can have significant effects on the percolation properties of the particle phase. For example, the percolation threshold is around 0.20 for ellipsoids of aspect ratio 3, whereas, in comparison, the percolation threshold for spheres is about 0.29 [10]. It is then naturally conjectured that the geometric shape can affect the percolation properties of the void phase as well. To test and verify this hypothesis is the main motivation of the present work.

For the void percolation of ellipsoids, the mathematical treatment of the interparticle connectivity is far more difficult than the sphere problems, due to the increased degrees of freedom for each particle. To the author's knowledge, there does not exist any mapping technique to reduce the problem into an equivalent Voronoi tessellation network. However, if the entire system is discretized into a fine mesh using sufficiently small pixels, then it is possible to map the original continuum system into its lattice equivalent with a high resolution. The determination of the characteristic properties of the void phase including percolation threshold and equivalent conductivity will be reduced to a traditional lattice problem, and the Monte Carlo simulation method can be used to identify these properties. In fact, the powerful computer technologies today enable the Monte Carlo modeling of percolation problems for nonspherical particles in a remarkably efficient way. Comparing with the 0.5 million words of computer memory used by Elam *et al.*'s work [18] two decades ago, the personal computers and workstations these days can easily handle gigabytes of memory allocation. When the mesh is sufficiently refined, one can obtain approximations of the exact percolation thresholds for both the material phase and the void space.

II. METHODS

A. Generation of random ellipsoids

A three-dimensional cubic simulation domain of unit size, namely, a "unit cell," was used to compute the void percolation of overlapping ellipsoids. To minimize the number of variables in the problem, spatially uncorrelated, equisized ellipsoids of revolution (with two geometric parameters: semiaxis length a and radius of revolution b) rather than generalized triaxial ellipsoids (with three geometric parameters) were under investigation. The ratio of the two semiaxis lengths of ellipsoid is defined as the "aspect ratio" in this study. The ellipsoids were generated from a Poisson process in which the centers and orientations of the particles followed a homogeneous distribution. In the spherical coordinate system, the axes of particles were oriented under a distribution function biased towards the z-axis, following the discussion by Yi and Sastry [10]. In order to minimize the boundary and scaling effects, the following treatments were applied during the generation process: (i) A sufficiently large number of ellipsoids ($\sim$100 000) were generated in the simulation domain. This placed a restriction on the particle diameter to around 0.04 at the onset of percolation, which is equivalent to 1/25 in terms of the ratio between the particle size and the simulation domain. When such a small particle-domain ratio is used, the boundary effects are negligible, per Yi and Sastry [19]. Therefore, periodic boundary conditions were not applied to the model since this would not induce any appreciable change in the result. (ii) The centers of ellipsoids were uniformly generated in a domain slightly larger than the unit cell to accommodate those particles that crossed the domain boundary but whose centers were located outside the cell, as shown in Fig. 1. This process was followed by the removal of the materials located outside the unit cell. Consequently, the void phase in the system was formed from the enclosures of the ellipsoidal surfaces.

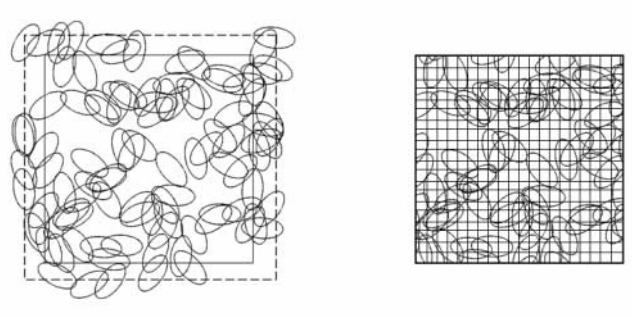

FIG. 1. Generation and discretization of random particles.

B. Discretization of the particulate system

The ellipsoidal system was then discretized into a three-dimensional uniform lattice, following a procedure similar to the digitalization of a picture. Let us denote each crossing point in the lattice as a "node." The location of each node relative to each ellipsoid was examined based on the mathematical equation of the ellipsoidal surface. The node was then assigned with a binary value, or "digitized," based on whether it was located in the interior of the particle. To make the algorithm more efficient, only those nodes in the vicinity of each ellipsoid were examined; that is, the ellipsoids were binned based on the extreme locations of their surface points. In the spherical coordinate system, if one denotes Δx, Δy, and Δz as the differences of extreme locations of an ellipsoid of revolution in the x, y, and z directions, respectively, then

$$\Delta x = 2\sqrt{b^2 \cos^2\theta \cos^2\varphi + b^2 \sin^2\varphi + a^2 \sin^2\theta \cos^2\varphi}, \tag{1}$$

$$\Delta y = 2\sqrt{b^2 \cos^2\theta \sin^2\varphi + b^2 \cos^2\varphi + a^2 \sin^2\theta \sin^2\varphi}, \tag{2}$$

$$\Delta z = 2\sqrt{a^2 \cos^2\theta + b^2 \sin^2\theta}, \tag{3}$$

where a is semiaxis length, b is radius of revolution, $\theta \in (0,\pi)$ is the elevation angle from the z axis and $\varphi \in (0,\pi)$ is the rotation angle about the z axis. Only those nodes located inside the "bin" encompassing each ellipsoid were checked for their locations relative to the ellipsoid. The next step was to remove the nodes located inside at least one of the ellipsoids. A site lattice network for the void space was then formed from the remaining nodes in the system. Appar-

ently the surface constructed in this way was not smooth geometrically because it was composed of block elements. However, when the mesh is sufficiently refined, the geometry will approach to the real void space. A converge test was made to illustrate the variation of the void union volume as a function of node number. This will be presented in the result section later.

C. Checking for conduction and percolation

Once the void space was mapped into a lattice network, the original continuum percolation system was reduced to a lattice percolation problem. The simulation scheme to check for percolation in such a lattice problem would be to search for a domain-crossing path that connects nodes from one side of the system to the opposite side. One way to do this would be to compute the equivalent conductivity in the corresponding thermal or electrical models. Specifically, in the thermal analysis, for example, a unit temperature difference can be prescribed on the two opposite surfaces of the system. Applying the finite element method, the reactive heat flux can then be computed as an approximation to the equivalent thermal conductivity. A zero equivalent conductivity indicates the onset of percolation in the system; otherwise, it is not percolated. However, finite element analysis typically demands large amounts of computer memory. This places a limitation on the applicability of the method especially when a high accuracy in the solution is required. Under the restriction of 32-bit computer memory allocation, for example, the maximum size of the model is approximately 200–300 elements per side of the unit cell. In view of this, a different method where an efficient algorithm adapted from the so-called burning algorithm [20,21] has been used to determine the percolation status of the resulting lattice network. Briefly, the nodes appearing on an arbitrary side of the unit cell were first identified. The connections between these nodes and the adjacent nodes in the system were then examined. The process was progressively repeated until no additional connections were found in the entire system. The system was detected as percolated if and only if such connections spanned to the opposite side of the domain. The advantage of this method lies in the fast speed and its independency of any commercial code.

A convergence test using various element numbers was performed for the problem of overlapping spheres. The estimated void percolation threshold for spheres was compared to the precise result found in literature. This test served as a validation procedure for the percolation searching algorithm developed in this study. The method was then extended to ellipsoids to obtain the void percolation threshold as a function of geometric aspect ratio. For each aspect ratio, percolation condition was examined at different volume fractions with equispaced intervals. Simulations using the same parameters were repeated for five times at each volume fraction. Those volume fractions (interpolated values) where the percolation was detected at a probability of 50% were recorded as percolated and the lowest volume fraction found percolated was identified as the "percolation threshold."

D. Scaling effects

Percolation threshold is always defined by default in the context of an infinite system. For a system of finite size, the onset of percolation is no longer deterministic and only a probability is available to describe the status of percolation. When we say a percolation threshold for a finite system, it is usually referred to the situation when the probability of percolation is 50%. Previous work showed that the continuum percolation probability in a finite domain varies with the ratio of the particle size and the domain [22]. From the scaling theories, it is possible to estimate the percolation threshold of an infinite domain based on the percolation probability of a finite system. In the current problem using a unit simulation cell, the scaling effects for determining percolation thresholds involve two parameters: (i) the size of particles (or, the total particle number in the simulation domain); (ii) the number of nodes (or elements) in the lattice network. Regarding the first effect, numerous works on the sphere problems using both analytical and simulation approaches can be found in literature. One of the main conclusions is that the percolation threshold varies linearly with N^{α} where N is the total number of spheres and α is a constant [23]. This finite-size scaling can be used to calculate the percolation properties for an infinite system. For the second effect, it turns out that the computed percolation threshold changes proportionally with element length, or $\gamma \propto 1/m$, where γ is the percolation threshold in terms of volume fraction; m is the element number along each side of the simulation domain.

In this study, a large number of particles were maintained in each simulation. As a consequence, the particle size effect was usually very small. When the particle aspect ratio is large, however, the finite size scaling effect is no longer negligible and it should be correlated to the major axis length of particle. In fact, in the extreme case where the particle length is greater than one, the system is always percolated regardless of the particle number. In view of this, the major axis length of particle was carefully maintained to be less than 1/6 in the present study. The effect of the element size (or, element number) was investigated via running the simulation under different element numbers while maintaining the particle size as constant. A curve of percolation threshold versus element number was then plotted to estimate the exact percolation threshold when the element number approaches to infinity.

It should be pointed out that the maximum element number under investigation was 1200 along each side of the unit cell, due to the restrictions of the available computer memory. This placed a limitation on the aspect ratio of particles since a reasonable number of elements must be present along the minor axis of particle meanwhile the major axis cannot be too long, as discussed previously. It has been found that it would be difficult to accurately determine the void percolation threshold for particles of aspect ratio greater than ten based on the current technique. Therefore the particle aspect ratio under investigation was limited to those values below ten.

III. RESULTS

A convergence test was performed on the union volume computation for the void space formed by overlapping spheres and ellipsoids. Figure 2 shows the void volume frac-

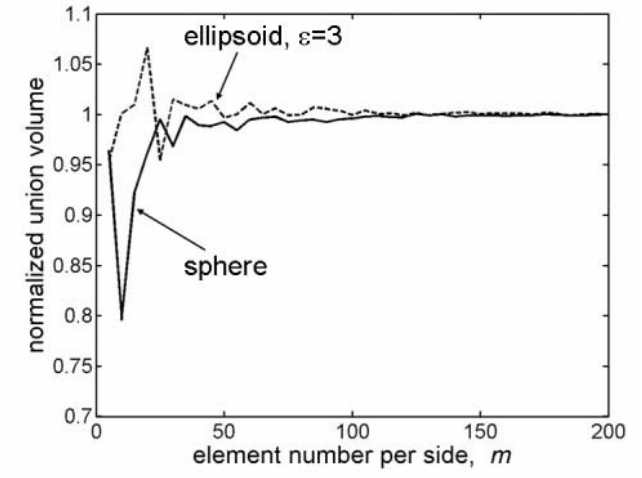

FIG. 2. Converging test for computation of the void volume fraction, using the discretization method. Particle number=4,000; the exact solution of the void volume fraction is 0.12.

tion as a function of element number m along each side of the simulation domain. Results for two aspect ratios 1 and 3 are presented. The void volume fraction was normalized by its exact solution, whose value was approximated as the computed volume fraction when $m=500$. It can be seen that both curves oscillate strongly at low m's, showing significant variations in coarse meshes. However, when the element number exceeds 50 or so, the oscillations in the curves become relatively mild and the estimated union volume is very close to the exact solution with a numerical error around 2–3 %. When the element number m is >100, the computed void volume fraction further approaches to its exact solution, with the error tolerance within 1%. Under the maximum element number $m=1200$ in the present study, there is no doubt that the computed volume fraction is considerably accurate.

Figure 3 is the visualization of the void space formed by 4000 monodisperse spheres having radius 0.05. The void system was discretized into approximately 15 000 elements, with element number 50 along each side of the unit cell. The volume fraction of the void system is ~12%. The finite element analysis was performed to compute the equivalent conductivity using the general-purpose commercial software ABAQUS. Unit material properties were assigned to each element, and a unit temperature difference was prescribed on two opposite faces of the model. Thermally insulated boundary conditions were specified on the rest surfaces. The contour plot in Fig. 3 displays the steady-state temperature distribution in the system. Since all the parameters were normalized to unit values, the reactive heat flux across either of the constrained surfaces was equivalent to the thermal conductivity of the whole system. The analysis was performed repeatedly for five times at six different volume fractions and the results are presented in Fig. 4. The short error bars in the figure indicate mild variations in the equivalent conductivity. (Apparently the standard variation is a function of the scaling effects, namely the number of particles and the number of elements.) At volume fraction 0.05, both the mean

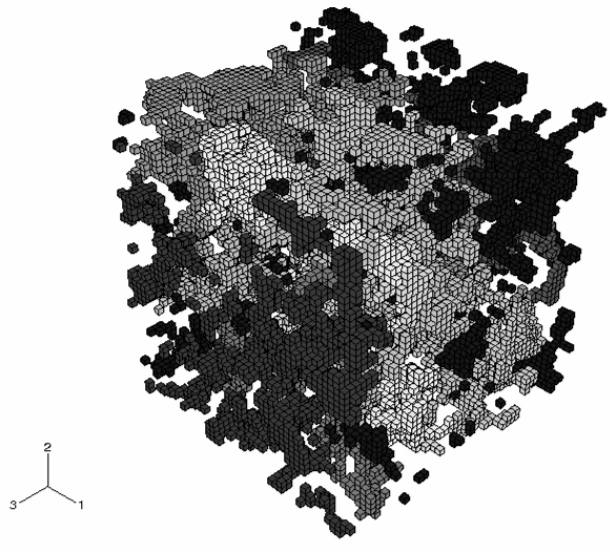

FIG. 3. Discretized void percolation system of spheres. Contour plot shows the temperature distribution for computing equivalent conductivity in the finite element analysis. Volume fraction of the void phase is 0.12; particle number=4000; sphere radius=0.04; element per side is 50; total element number≈15 000.

value and the standard deviation of the computed conductivity are zero, implying that the critical volume fraction of percolation for spheres is located somewhere between 0.05 and 0.1. Note that the element number $m=50$ was used in the computation for Fig. 4. Further studies using larger m's (up to 200) revealed that the void percolation threshold was in the vicinity of 0.05. Compared to the precise result of 0.03 found in the literature, this computed solution is apparently overestimated due to the insufficient element number used in the finite element analysis. It has been concluded that, in general, it is not very accurate to use the finite element method to identify the percolation threshold in void percolation problems, due to the complexity in matrix operations as

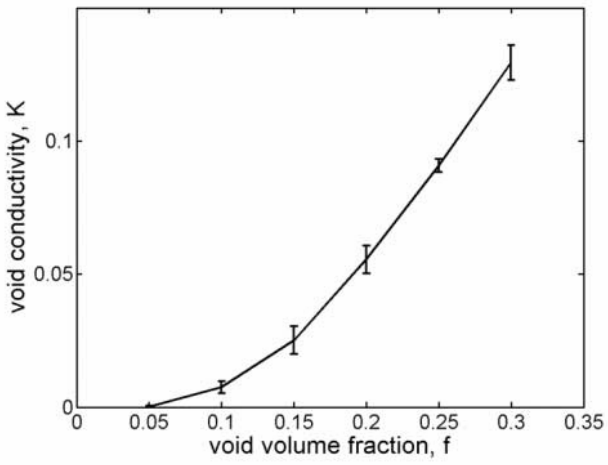

FIG. 4. Equivalent conductivity of the void phase as a function of void volume fraction. The parameters used here are the same as in Fig. 3.

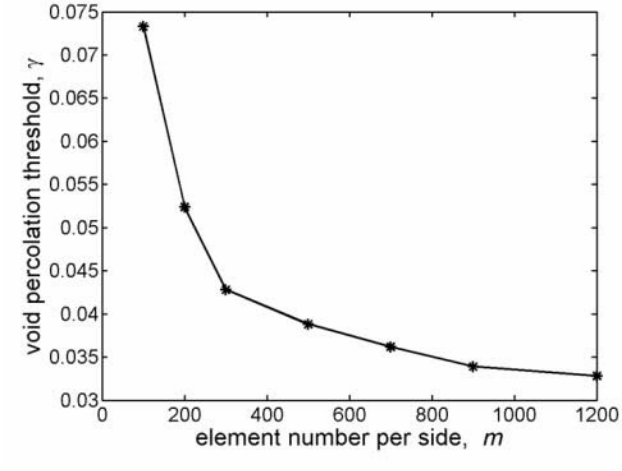

FIG. 5. Computed void percolation threshold of spheres as a function of element number m.

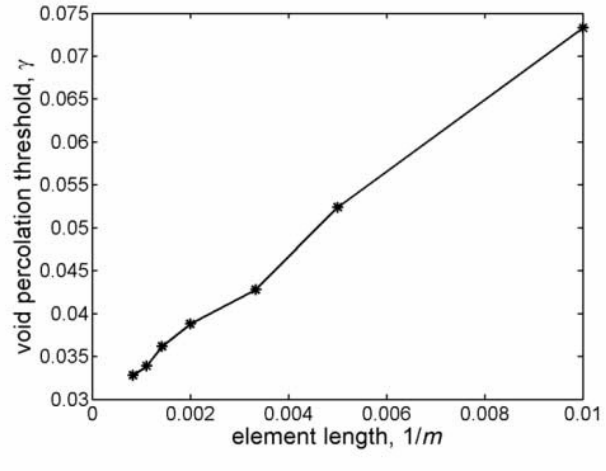

FIG. 6. Computed void percolation threshold of spheres as a function of element length $1/m$.

well as the restrictions on computer memory. Nevertheless, the solution routines in this method are convenient to implement and they do not require additional algorithms. In addition, low resolution is relevant to the percolation threshold only (at very low volume fraction), not the conductivity of percolated systems (at higher volume fractions). Thus, it is helpful to apply the method in those situations where conductive property is the main interest.

Figure 5 shows convergence testing on the lattice percolation algorithm for determining the void percolation threshold of overlapping spheres. It should be noted that this algorithm is different from the finite element method used for conduction computation. Different element numbers ranging from 100 to 1200 elements per side of the simulation domain were used in Fig. 5. At $m=100$, the computed void percolation threshold γ is 0.073 in terms of volume fraction of the void phase. When $m=200$ is used, this value becomes 0.052, showing substantial improvement in the solution accuracy. For $m=1{,}200$, the detected percolation threshold is 0.0328, which comes very close to the precise solution 0.0301. The curve will be asymptotic to the exact percolation threshold γ_c when $m\rightarrow\infty$. To identify this asymptotic solution, the computed percolation threshold was plotted as a function of element length, or $1/m$, as shown in Fig. 6. Clearly, the relation between γ and $1/m$ approximately forms a straight line. By linear extrapolation, the percolation threshold at $1/m=0$ (that is, the y intercept of the curve) was identified as $\gamma_c=0.0294$. This value was slightly underestimated compared to the precise result 0.0301. However, this resolution should be considered acceptable due to the approximating nature of the discretization method.

By applying the same technique to ellipsoids, the asymptotic value of the void percolation threshold γ_c (that is, the extrapolated γ when $m\rightarrow\infty$) for ellipsoids of revolution was estimated for several different aspect ratios ranging from 1 to 8, as shown in Fig. 7. From this curve, it is clear that the threshold does not possess a constant value. In fact, the estimated void percolation threshold increases monotonically with the aspect ratio. For example, the void percolation threshold rises from 0.0294 to 0.0325 when the aspect ratio increases from 1 to 2. For ellipsoids of aspect ratio 8, the percolation threshold becomes 0.0412, which is about 40% higher than that of sphere. This is undoubtedly a nonnegligible difference, confirming that one must deal with spheres and ellipsoids separately when the void percolation problems are under investigation. It is still unclear if the void percolation threshold will reach an asymptotic and finite value when the aspect ratio of ellipsoid approaches infinity. This requires further studies in future.

IV. CONCLUSION

The void percolation and conduction problems involving equisized overlapping ellipsoids of revolution were studied using the discretization method. The void percolation threshold for ellipsoids was determined as a function of particulate

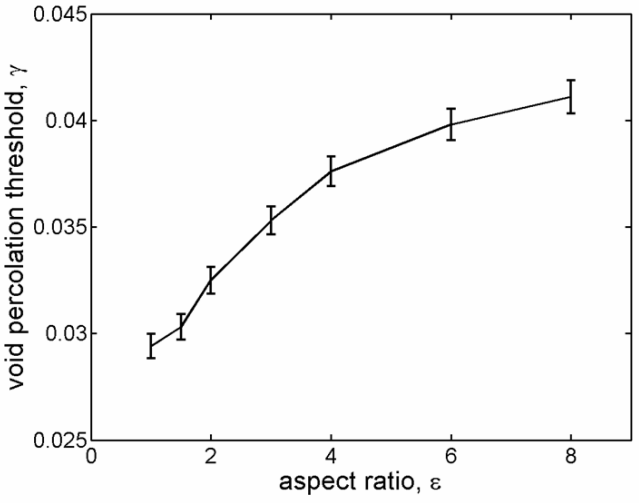

FIG. 7. Void percolation threshold (extrapolated values for zero element length) as a function of ellipsoid aspect ratio.

aspect ratio. The estimated percolation threshold of spheres was compared to the precise result found in the literature, showing good agreement. The equivalent conductivity was also estimated from the finite element analysis. These results indicate that there are no universal constants for void percolation threshold or conductivity for particulate systems. Therefore, the results obtained from systems consisting of spheres cannot be applied to problems involving ellipsoidal particles in general. This is true for not only the traditional continuum percolation systems but also the void percolation problems. In addition, it should be pointed out that evaluation of conductive properties is closely related to the void percolation problem in the current work because both involve the same discretization method. They reveal the particle connectivity at different material densities: the computation of void percolation threshold is relevant to the connectivity at low volume fractions of the void phase, whereas the conductivity computation is an effective way to evaluate the connectivity in a percolated system at higher volume fractions.

[1] S. R. Broadbent and J. M. Hammersly, Proc. Cambridge Philos. Soc. **53**, 629 (1957).
[2] C. W. Wang, X. Cheng, A. M. Sastry, and S. B. Choi, J. Eng. Mater. Technol. **121**, 503 (1999).
[3] S. Datta and S. Redner, Int. J. Mod. Phys. C **9**, 1535 (1998).
[4] S. Mohanty and M. Sharma, Phys. Lett. A **154**, 475 (1991).
[5] Y. B. Yi, L. M. Berhan, and A. M. Sastry, J. Appl. Phys. **96**, 1318 (2004).
[6] M. F. Sykes and J. W. Essam, Phys. Rev. Lett. **10**, 3 (1963).
[7] G. E. Pike and C. H. Seager, Phys. Rev. B **10**, 1421 (1974).
[8] S. W. Haan and R. Zwanzig, J. Phys. A **10**, 1547 (1977).
[9] A. Coniglio, U. Deangelis, A. Forlani, and G. Lauro, J. Phys. A **10**, 219 (1977).
[10] Y. B. Yi and A. M. Sastry, Proc. R. Soc. London, Ser. A **460**, 2353 (2004).
[11] S. Kirkpatrick, Rev. Mod. Phys. **45**, 574 (1973).
[12] S. Torquato, *Random Heterogeneous Materials* (Springer-Verlag, New York, 2002).
[13] X. Cheng and A. M. Sastry, Mech. Mater. **31**, 765 (1999).
[14] A. Klemm, R. Kimmich, and M. Weber, Phys. Rev. E **63**, 041514 (2001).
[15] A. R. Kerstein, J. Phys. A **16**, 3071 (1983).
[16] M. D. Rintoul, Phys. Rev. E **62**, 68 (2000).
[17] S. C. van der Marck, Phys. Rev. Lett. **77**, 1785 (1996).
[18] W. T. Elam, A. R. Kerstein, and J. J. Rehr, Phys. Rev. Lett. **52**, 1516 (1984).
[19] Y. B. Yi, C. W. Wang, and A. M. Sastry, J. Electrochem. Soc. **151**, A1292 (2004).
[20] D. Dhar, Phys. Rev. Lett. **64**, 1613 (1990).
[21] P. Bak and K. Chen, Physica D **38**, 5 (1989).
[22] Y. B. Yi and A. M. Sastry, Phys. Rev. E **66**, 066130 (2002).
[23] D. Stauffer and A. Aharony, *Introduction to Percolation Theory*, 2nd ed. (Taylor & Francis, Bristol, 1992).